Temperature-Dependent Variations and Intraspecies Diversity of the Structure of the Lipopolysaccharide of *Yersinia pestis*[†,‡]

Yuriy A. Knirel,[§] Buko Lindner,[#] Evgeny V. Vinogradov,[§,⊥] Nina A. Kocharova,[§] Sof'ya N. Senchenkova,[§] Rima Z. Shaikhutdinova,[∥] Svetlana V. Dentovskaya,[∥] Nadezhda K. Fursova,[∥] Irina V. Bakhteeva,[∥] Galina M. Titareva,[∥] Sergey V. Balakhonov,[○] Otto Holst,[#] Tat'yana A. Gremyakova,[∥] Gerald B. Pier,*[,&] and Andrey P. Anisimov[∥]

N. D. Zelinsky Institute of Organic Chemistry, Russian Academy of Sciences, Moscow 119991, Russia, Research Center Borstel, Leibniz Center for Medicine and Biosciences, D-23845 Borstel, Germany, State Research Center for Applied Microbiology, Obolensk 142279, Moscow Region, Russia, Antiplague Research Institute of Siberia and Far East, Irkutsk 664047, Russia, and Channing Laboratory, Brigham and Women's Hospital, Harvard Medical School, Boston, Massachusetts 02115

Received July 22, 2004; Revised Manuscript Received October 18, 2004

ABSTRACT: *Yersinia pestis* spread throughout the Americas in the early 20th century, and it occurs predominantly as a single clone within this part of the world. However, within Eurasia and parts of Africa there is significant diversity among *Y. pestis* strains, which can be classified into different biovars (bv.) and/or subspecies (ssp.), with bv. orientalis/ssp. *pestis* most closely related to the American clone. To determine one aspect of the relatedness of these different *Y. pestis* isolates, the structure of the lipopolysaccharide (LPS) of four wild-type and one LPS-mutant Eurasian/African strains of *Y. pestis* was determined, evaluating effects of growth at mammalian (37 °C) or flea (25 °C) temperatures on the structure and composition of the core oligosaccharide and lipid A. In the wild-type clones of ssp. *pestis*, a single major core glycoform was synthesized at 37 °C whereas multiple core oligosaccharide glycoforms were produced at 25 °C. Structural differences occurred primarily in the terminal monosaccharides. Only tetraacyl lipid A was made at 37 °C, whereas at 25 °C additional pentaacyl and hexaacyl lipid A structures were produced. 4-Amino-4-deoxyarabinose levels in lipid A increased with lower growth temperatures or when bacteria were cultured in the presence of polymyxin B. In *Y. pestis* ssp. *caucasica*, the LPS core lacked D-*glycero*-D-*manno*-heptose and the content of 4-amino-4-deoxyarabinose showed no dependence on growth temperature, whereas the degree of acylation of the lipid A and the structure of the oligosaccharide core were temperature dependent. A spontaneous deep-rough LPS mutant strain possessed only a disaccharide core and a slightly variant lipid A. The diversity and differences in the structure of the *Y. pestis* LPS suggest important contributions of these variations to the pathogenesis of this organism, potentially related to innate and acquired immune recognition of *Y. pestis* and epidemiologic means to detect, classify, control and respond to *Y. pestis* infections.

Bubonic and pneumonic plague is caused by the Gram-negative bacterium *Yersinia pestis* circulating in natural foci in Eurasia, Africa, and the Americas, which involve a rodent reservoir and an insect vector (*1*−*7*). Enzootic *Y. pestis* infection is due to continual transmission among susceptible rodents by various flea vectors, which results in acute infection with bacteremia in their enzootic rodent hosts. The high lethality of plague in rodent reservoirs is necessary for the organism's continued transmission in nature. Fleas ingesting infected blood during preagonal bacteremia must depart from the host and feed on a new rodent, which subsequently becomes infected (*1*−*7*). It has been assumed that selective pressures within different host species and fleas contribute to the emergence of variant strains of *Y. pestis* which have been variously classified as biovars (bv.), based on differences in glycerol fermentation, nitrate reduction, and ammonia oxidation, or as subspecies (ssp.) or ecotypes (*4*), wherein strains are differentiated due to variations in fermentative activity, nutritional requirements, and ability to cause infectious bacteremia and death in diverse mammalian species.

The pathogenicity of *Y. pestis* is determined, in part, by a number of bacterial features that counteract mammalian (*1*−*8*) and insect (*1, 2, 5*−*9*) antimicrobial factors, ensuring

[†] Research performed within the framework of the International Science and Technology Center (ISTC) Partner Project #1197, supported by the Cooperative Threat Reduction Program of the US Department of Defense (ISTC Partner). Research also supported by the Russian Ministry for Industry, Science and Technology Contract #43.600.1.4.0031 and the German Research Foundation Grant LI-448-1.

[‡] Different parts of this work were presented at the eighth International Symposium on *Yersinia*, September 4-8, 2002 in Turku, Finland, the 12th European Carbohydrate Symposium, July 6-12, 2003 in Grenoble, France, and the 104th General ASM Meeting, May 23-27, 2004 in New Orleans, LA.

* Corresponding author. Mailing address: Channing Laboratory, 181 Longwood Av., Boston, MA 02115. Telephone: 617-525-2269. Fax: 617-525-2510. E-mail: gpier@rics.bwh.harvard.edu.-

[§] Zelinsky Institute of Organic Chemistry.

[#] Leibniz Center for Medicine and Biosciences.

[⊥] Present address: Institute for Biological Sciences, National Research Council, 100 Sussex Dr., Ottawa ON, Canada K1A 0R6.

[∥] State Research Center for Applied Microbiology.

[○] Antiplague Research Institute of Siberia and Far East.

[&] Harvard Medical School.

10.1021/bi048430f CCC: $30.25
Published on Web 01/08/2005

Table 1: *Y. pestis* Strains Used in These Studies

strain	biovar/subspecies[a]	relevant characteristics	geographical origin of the parent strain
KM218	orientalis/*pestis*	pFra$^-$, pCD$^-$, pPst$^-$, Δ*pgm*; derived from the Russian vaccine strain EV line NIIEG	Madagascar
EV11M	antiqua/*pestis*	pFra$^-$, pCD$^-$, pPst$^-$, Δ*pgm*; derived from the Russian vaccine strain EV line NIIEG and carrying undefined chromosomal mutation(s) resulting from multiple in vitro passages	Madagascar
KM260(11)	antiqua/*pestis*	pFra$^-$, pCD$^-$, pPst$^-$; derived from the virulent strain 231	Aksai focus, Kirghizia
KIMD1	medievalis/*pestis*	pFra$^-$, pCD$^-$, pPst+	Iran/Kurdistan
1146	antiqua/*caucasica*	pFra$^-$, pCD$^-$, pPst$^-$; derived from the virulent strain 1146	Trans-Caucasian-highland focus, Caucasus

[a] For more detailed information on biovar-subspecies interrelations see ref. (*4*).

maintenance of the pathogen in these hosts during the transmission cycle. One of these is the lipopolysaccharide (LPS),[1] a virulence factor of many Gram-negative bacteria. LPS consists of three parts: lipid A, a core oligosaccharide, and an O-specific polysaccharide (O-antigen) whose synthesis gives rise to the smooth form of this structure. *Y. pestis* has a rough-type LPS (*10*−*15*) lacking the O-polysaccharide chain due to the nonfunctionality of the O-antigen gene cluster as a result of several frame-shift mutations (*13, 14*). In contrast, the enteropathogenic *Yersinia* species *Yersinia pseudotuberculosis* and *Yersinia enterocolitica*, which cause chronic intestinal infections, possess a smooth-type LPS, which does not confer resistance to the bactericidal action of human serum (*16*) and antimicrobial peptides (*17*).

In mammals, the *Y. pestis* LPS mediates endotoxic shock via induction of potent cytokines whose production is balanced, in part, by the ability of the V antigen encoded on pCD to provoke production of the antiinflammatory cytokine, interleukin-10 (IL-10) (*18*) as well as bind to toll-like receptor 2 which may provide a pro-inflammatory stimulus as well. Because IL-10 production, like that of most cytokines made during infection can be cyclic (*19*), it is likely that LPS-induced inflammatory cytokines significantly contribute to the host's death when the effects of IL-10 are insufficient to counteract the effects of LPS (*3, 20*). LPS also seems to play a role in resistance of *Y. pestis* to serum-mediated lysis (*16*), which is necessary for survival and growth of the bacteria in mammalian blood (*2*−*7, 9*). However, as opposed to the majority of *Y. pestis* strains, some natural isolates of ssp. *caucasica* are highly susceptible to the bactericidal action of normal human serum (*4*), suggesting differences in the LPS structure of this variant *Y. pestis* ssp. The *Y. pestis* LPS structure also determines bacterial resistance to cationic antimicrobial peptides (*17*), a key component of innate immunity in both mammals and insects (*21*). Again, representatives of ssp. *caucasica*, as well as those of ssp. *hissarica* and fresh isolates of ssp. *altaica*, are highly sensitive to polymyxin B (*4*). *Y. pestis* strains belonging to all ssp. are highly lethal for mice and the overwhelming majority of ssp. *pestis* isolates are also lethal for guinea pigs, whereas strains of ssp. *caucasica*, *hissarica*, and *altaica* are usually of low virulence or even avirulent in guinea pigs (*4*).

[1] Abbreviations: Ara4N, 4-amino-4-deoxyarabinose; CSD, capillary skimmer dissociation; DD-Hep, D-*glycero*-D-*manno*-heptose; LD-Hep, L-*glycero*-D-*manno*-heptose; FT−ICR ESI MS, Fourier transform-ion cyclotron resonance electrospray ionization mass spectrometry; gHSQC, gradient-selected heteronuclear single-quantum coherence; Kdo, 3-deoxy-D-*manno*-oct-2-ulosonic acid; Ko, D-*glycero*-D-*talo*-oct-2-ulosonic acid; LA, lipid A.; LPS, lipopolysaccharide; OS, oligosaccharide; PMB, polymyxin B.; ROESY, rotating-frame nuclear Overhauser effect spectroscopy.

Recently, the structure of the *Y. pestis* LPS has been extensively studied. The full lipid A structure (*22, 23*), a partial core structure of one strain (*11*), and preliminary data on the full structure of the LPS oligosaccharide from another strain (*15, 24*) have been published. The lipid A structure in *Y. pestis* bv. orientalis has been found to depend on the growth temperature and suggested to have biological significance in regard to transmission in fleas and mammals (*23*). However, no comprehensive analysis of the *Y. pestis* LPS structure, including both lipid A and substituent oligosaccharide structures synthesized by various *Y. pestis* strains differing in their geographical occurrence and epidemiologic significance has been reported. Here we describe results from studies of the structure of the LPS from strains of *Y. pestis* ssp. *pestis* (consisting of bvs. orientalis, antiqua, and medievalis) and ssp. *caucasica* (bv. antiqua) grown at different cultivation temperatures, which lead to distinct changes in the structure of this key pathogenic factor. In addition, we have characterized the LPS structure of a mutant strain EV11M, which is susceptible to compelement and antimicrobial peptides in order to determine whether these biologic properties are associated with changes in the LPS structure.

EXPERIMENTAL PROCEDURES

Bacterial Strains. Y. pestis strain KIMD1 was kindly ptovided by Dr. M. Skurnik (University of Turku, Turku, Finland). Other *Y. pestis* strains used were obtained from the Russian Research Anti-Plague Institute "Microbe" (Saratov, Russia). Characteristics of the strains are given in Table 1. To guarantee the safety of the investigators, *Y. pestis* strains were attenuated by elimination of the virulence plasmid, pCD (*7*). None of the absent plasmids or missing parts of the genome contained genes for LPS biogenesis in any of the strains except for strain EV11M. All parental strains were virulent in both mice and guinea pigs, except for strain 1146, which is virulent in mice and avirulent in guinea pigs. Bacterial cultures were started from lyophilized stocks.

Growth of Bacteria. For LPS isolation, the strains were grown at 37 or 25 °C in New Brunswick Scientific fermentors with working volumes up to 10 L of liquid aerated media. Growth medium was composed of fish-flour hydrolysate (20−30 g/L), yeast autolysate (10 g/L), glucose (3−9 g/L), K_2HPO_4 (6 g/L), KH_2PO_4 (3 g/L), and $MgSO_4$ (0.5 g/L); pH 6.9−7.1. pH and pO_2 control was used with a specified pO_2 value >10%. For some LPS preparations, polymyxin B (AppliChem GmbH, Germany) was added to the nutrient medium to a final concentration of 20 U/mL. Biomasses were harvested by centrifugation after 48 h of

incubation and then lyophilized. Solid agar medium was prepared by adding 2% agar, pH 7.2 to the liquid medium.

Isolation of LPS and SDS−PAGE. LPS was extracted from dried cells with phenol/chloroform/light petroleum ether (*25*), enzymatically digested first with nucleases then proteases, and further purified by repeated ultracentrifugation (105 000*g*, 4 h). The purity of the isolated LPS preparations was evident from the lack of protein contamination assessed by gel electrophoresis and nucleic acid contamination as determined by sugar composition analysis (see below). A smooth-type LPS of *Escherichia coli* O55:B5 (Sigma) was used as a control in some assays. The LPS preparations extracted from different *Y. pestis* cultures grown at 25 °C or 37 °C are designated as LPS-25$_{<\text{strain no.}>}$ or LPS-37$_{<\text{strain no.}>}$ or, when appropriate, <strain no.>-25 or <strain no.>-37, respectively.

SDS−glycine polyacrylamide gel electrophoresis and silver staining of the gels were performed as described (*13*).

Mild Acid Degradation. LPS-25 and LPS-37 from each strain were degraded with aqueous 2% HOAc at 100 °C for 4 h. The water-insoluble lipid precipitates (crude lipid A) were separated by centrifugation (12000*g*, 15 min), washed with water, suspended in water, and lyophilized, and the solid preparations were then extracted with a chloroform−methanol mixture (1:1, v/v), which extracts free phospholipids from lipid A. The lipid A preparations are designated as LA-25$_{<\text{strain no.}>}$ and LA-37$_{<\text{strain no.}>}$ as per the designations for the initial LPS preparations.

The water-soluble supernatants from the wild-type-LPS strains *Y. pestis* KM218, KM260(11), KIMD1, and 1146 were fractionated by gel-permeation chromatography on a column of Sephadex G-50 (S) (70 × 2.6 cm; Amersham Biosciences, Sweden) using aqueous 1% HOAc supplemented with 0.4% pyridine as eluant. The supernatants from *Y. pestis* EV11M were fractionated by gel-permeation chromatography on a column of TSK HW-40 (S) (75 × 1.6 cm; Merck, Germany) in aqueous 1% HOAc. Monitoring was performed with a differential refractometer (Knauer, Germany). Fractions that contained core oligosaccharides (OSs) were collected and lyophilized. The OSs are designated as OS-25$_{<\text{strain no.}>}$ and OS-37$_{<\text{strain no.}>}$ similar to the designations of the initial LPS preparations.

Fractionation of the oligosaccharide from *Y. pestis* KM218 was achieved by anion-exchange chromatography on a HiTrap Q column (5 mL; Amersham Biosciences, Sweden) using water to elute neutral contaminants (fraction I) and then a 0 → 1 M gradient of NaCl in water to elute two fractions, designated II and III, which were subsequently desalted on Sephadex G-15. Fraction III from LPS-25 of *Y. pestis* KM218 was reduced by treatment with $NaBH_4$ in water and further fractionated by high-performance anion-exchange chromatography on a semipreparative column of CarboPac PA100 (250 × 9 mm; Dionex, USA) in a 0.05 → 0.5 M gradient of NaOAc in 0.1 M NaOH at 3 mL/min over 1 h. Fractions of 3 mL were collected and analyzed on an analytical column of CarboPac PA100 (250 × 4.6 mm; Dionex, USA) using the same gradient run at 1 mL/min.

Composition and Methylation Linkage Analyses. Sugar analysis was performed by gas−liquid chromatographic (GLC) separation of monosaccharides and identification of the sugar monomers that had been derivitized to alditol acetates (*26*). Hydrolysis of the LPS oligosaccharide was performed with 2 M CF_3CO_2H (4 h, 100 °C) followed by conventional reduction with $NaBH_4$ and acetylation with Ac_2O in pyridine (1:1.5, v/v; 100 °C, 30 min). GLC of the derived alditol acetates was carried out using a Hewlett-Packard 5880 chromatograph (Avondale, PA) equipped with a DB-5 fused-silica capillary column (30 m × 0.25 mm) and a temperature program of 160 °C (1 min) → 260 °C at 3 °C/min. Amino components were analyzed after hydrolysis with 4 M HCl (100 °C, 16 h), using a Biotronik LC-2000 amino acid analyzer equipped with a column (0.4 × 22 cm) of Ostion LG AN B cation-exchange resin in 0.2 M sodium citrate buffer, pH 3.25, at 80 °C.

For detection of 3-deoxy-D-*manno*-oct-2-ulosonic acid (Kdo), D-*glycero*-D-*talo*-oct-2-ulosonic acid (Ko) and 4-amino-4-deoxyarabinose (Ara4N), the acetylated methyl glycosides were prepared by methanolysis of the LPS with 2 M HCl in methanol (45 min or 16 h, 85 °C). After removal of the solvent the products were acetylated with Ac_2O in pyridine (1:1.5, v/v, 85 °C, 20 min) and analyzed by GLC−MS on a Hewlett-Packard HP 5989A instrument equipped with a 30-m HP-5MS column (Hewlett-Packard) using a temperature gradient 150 °C (3 min) → 320 °C at 5 °C/min. Ammonia was used as reactant gas in chemical ionization MS.

For fatty acid analysis, lipid A was methanolyzed with 2 M HCl in methanol (85 °C, 16 h), and after evaporation of the solvent the product was acetylated with Ac_2O in pyridine (1:1.5, v/v, 85 °C, 20 min) and analyzed by GLC−MS on a HP-5MS as described above.

For linkage analysis, the OS was methylated with CH_3I in Me_2SO in the presence of sodium methylsulfinylmethanide (*27*), and hydrolysis was performed as for the sugar analysis. The partially methylated monosaccharides were reduced with $NaBD_4$, subsequently converted to the alditol acetates and analyzed by GLC−MS as described above.

NMR Spectroscopy. Prior to measurements, samples were exchanged twice with D_2O. ^1H and ^{13}C NMR spectra were recorded on a Varian Inova 500 spectrometer in D_2O solutions at 25 °C with acetone as an internal standard (δ_H 2.225, δ_C 31.5 ppm). Standard pulse sequences were used in two-dimensional NMR experiments, including COSY, TOCSY (mixing time 120 ms), ROESY (mixing time 250 ms), and $^1H,^{13}C$ gHSQC. Spectra were assigned using the computer program Pronto (*28*).

Mass Spectrometry. High-resolution electrospray ionization Fourier transform ion cyclotron resonance (ESI FT−ICR) MS was performed in the negative ion mode using an ApexII-instrument (Bruker Daltonics, Billerica, MT) equipped with a 7 T actively shielded magnet and an Apollo electrospray ion source. Mass spectra were acquired using standard experimental sequences as provided by the manufacturer. Samples were dissolved at a concentration of ∼ 10 ng/μL in a 50:50:0.001 (v/v/v) mixture of 2-propanol, water, and triethylamine and sprayed at a flow rate of 2 μL/min. Capillary entrance voltage was set to 3.8 kV, and dry gas temperature to 150 °C. Capillary skimmer dissociation (CSD) was induced by increasing the capillary exit voltage from −100 to −350 V. The spectra were charge deconvoluted, and the mass numbers given refer to the monoisotopic molecular masses.

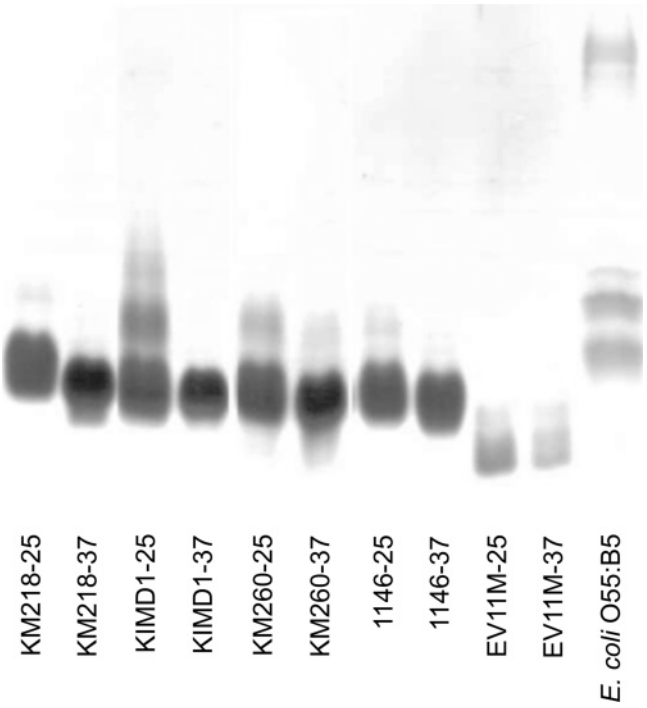

FIGURE 1: Silver-stained SDS−PAGE of LPS samples from *Y. pestis* strains grown at 25 °C or 37 °C. LPS from *E. coli* O55:B5 is shown for comparison. Here, 2.5 μg of each *Y. pestis* LPS and 5 μg of the *E. coli* LPS were applied to the gel. Distinctions between the mobility of the LPS samples are maximally seen when the upper confines of the spots are compared.

RESULTS

Isolation and Characterization of the LPS from Y. pestis. Each *Y. pestis* strain was cultivated at 25 and 37 °C, and the corresponding lipopolysaccharides (LPS-25 and LPS-37) were isolated by phenol/chloroform/light petroleum extraction and studied by SDS−PAGE (Figure 1). There were no significant distinctions in mobility of the LPS samples from *Y. pestis* ssp. *pestis* strains KM218, KM260(11), KIMD1 and *Y. pestis* ssp. *caucasica* strain 1146, but LPS preparations from strains grown at 37 °C migrated through the gel slightly faster and as more compact bands compared to the migration of LPS synthesized at 25 °C, suggesting that LPS-25 molecules are on average bigger than those of LPS-37.

The LPS-25 and LPS-37 from a known mutant strain, *Y. pestis* EV11M, derived by repeated serial passage from the same parental strain as KIM218, migrated much faster in the SDS gels (Figure 1). This finding indicated that one effect of the mutations introduced into this strain resulted in a LPS with a smaller oligosaccharide compared with other *Y. pestis* strains.

GLC−MS of the acetylated derivatives obtained after methanolysis of the LPS from all strains studied revealed the presence of Kdo, Ko, and Ara4N. In addition, a derivative of a Ko−Kdo disaccharide was identified by the presence of a $[M - CO_2Me]^+$ ion at *m*/*z* 793 and typical fragmentation ions for Kdo at the reducing end (*m*/*z* 375) and Ko at the nonreducing end (*m*/*z* 461) in electron impact MS (*29*). The Ko−Kdo disaccharide structure was further confirmed by the presence of a $[M + 18]^+$ ammonium-adduct ion at *m*/*z* 870 in chemical ionization MS (for the electron impact mass spectrum and explanation of diagnostic ions see Supporting Information).

Table 2: Sugar Analysis of Core Oligosaccharides from the LPS of Wild-Type-LPS *Y. Pestis* Strains[a]

	Y. pestis ssp. *pestis* KM218		*Y. pestis* ssp. *caucasica* 1146	
monosaccharide	OS-25	OS-37	OS-25	OS-37
D-glucose	1	1	1	1
D-galactose	0.4		0.9	0.4
L-*glycero*-D-*manno*-heptose[b]	2.3	2.6	2.7	2.6
D-*glycero*-D-*manno*-heptose	0.4	0.8		
D-glucosamine	0.6	0.8	0.2	0.4

[a] Given is the GLC detector response of the acetylated alditol relative to glucose. [b] Sum of derivatives of heptose and 1,6-anhydroheptose.

Isolation and compositional analysis of the oligosaccharides from the LPS of Y. pestis. Oligosaccharides were isolated by mild acid hydrolysis followed by gel permeation chromatography from the LPS of one *Y. pestis* ssp. *pestis* strain, KM218, and one *Y. pestis* ssp. *caucasica* strain, 1146, as well as from the rapidly migrating LPS of the mutant strain EV11M. The LPS from the *Y. pestis* ssp. *pestis* and ssp. *caucasica* strains gave mixtures of oligosaccharides (OS-25 and OS-37) composed of hexa- to octasaccharides, whereas the oligosaccharide from *Y. pestis* mutant strain EV11M was a disaccharide, consistent with the migration properties of the LPS in the SDS−PAGE.

Sugar analysis of OS-25_{218} from *Y. pestis* ssp. *pestis* by GLC−MS of the acetylated alditols derived after full acid hydrolysis revealed glucose, galactose, L-*glycero*-D-*manno*-heptose (LD-Hep), D-*glycero*-D-*manno*-heptose (DD-Hep) and 2-amino-2-deoxyglucose (GlcN) in the ratios 1:0.4:2.3:0.4:0.6 (Table 2). OS-37_{218} contained the same monosaccharides but no galactose, the content of DD-Hep being higher than in OS-25_{218} (Table 2). OS-25_{1146} and OS-37_{1146}, isolated from *Y. pestis* ssp. *caucasica*, differed by the absence of DD-Hep and a lower content of GlcN, the content of Gal being higher in OS-25_{1146} than in OS-37_{1146} (Table 2). Thus, there were clear differences in the oligosaccharides obtained from the LPS of these two different *Y. pestis* ssp.

None of these monosaccharides, nor other neutral or amino sugar monomers were found in either OS-25_{EV11M} or OS-37_{EV11M} from the *Y. pestis* EV11M LPS, and thus the oligosaccharide from this strain is a disaccharide(s) composed of only Kdo and Ko.

Mass Spectrometric Analysis of the Oligosaccharides from Y. pestis ssp. pestis strain KM218. The negative ion ESI FT−ICR mass spectrum of OS-37_{218} (Figure 2A) showed one major peak at *m*/*z* 1371.45, which was in excellent agreement with a heptasaccharide composed of $GlcNAc_1Glc_1Hep_4Kdo_1$ (compound **1a**, calculated molecular mass 1371.45 Da). There was also a minor satellite peak at *m*/*z* 1353.45 ($\Delta m/z$ −18) for the same compound indicating the presence of some Kdo in an anhydro from. A second minor peak (~10%) was present at *m*/*z* 1168.38 ($\Delta m/z$ −203) that corresponded to compound **1a** lacking GlcNAc (compound **1a′**); it was thus estimated that GlcNAc is present in ~90% of the molecules. A third minor peak was present at *m*/*z* 1607.52 ($\Delta m/z$ +236), indicating the presence in OS-37_{218} of molecules with an additional Ko residue (compound **1c**).

The negative ion ESI FT−ICR mass spectrum of OS-25_{218} (Figure 2B) was more complex and showed four series of major ions for compounds **1a**, **1b**, **1c** and **1d**. The ion for **1a** in the mass spectrum of OS-25_{218} had the same molecular

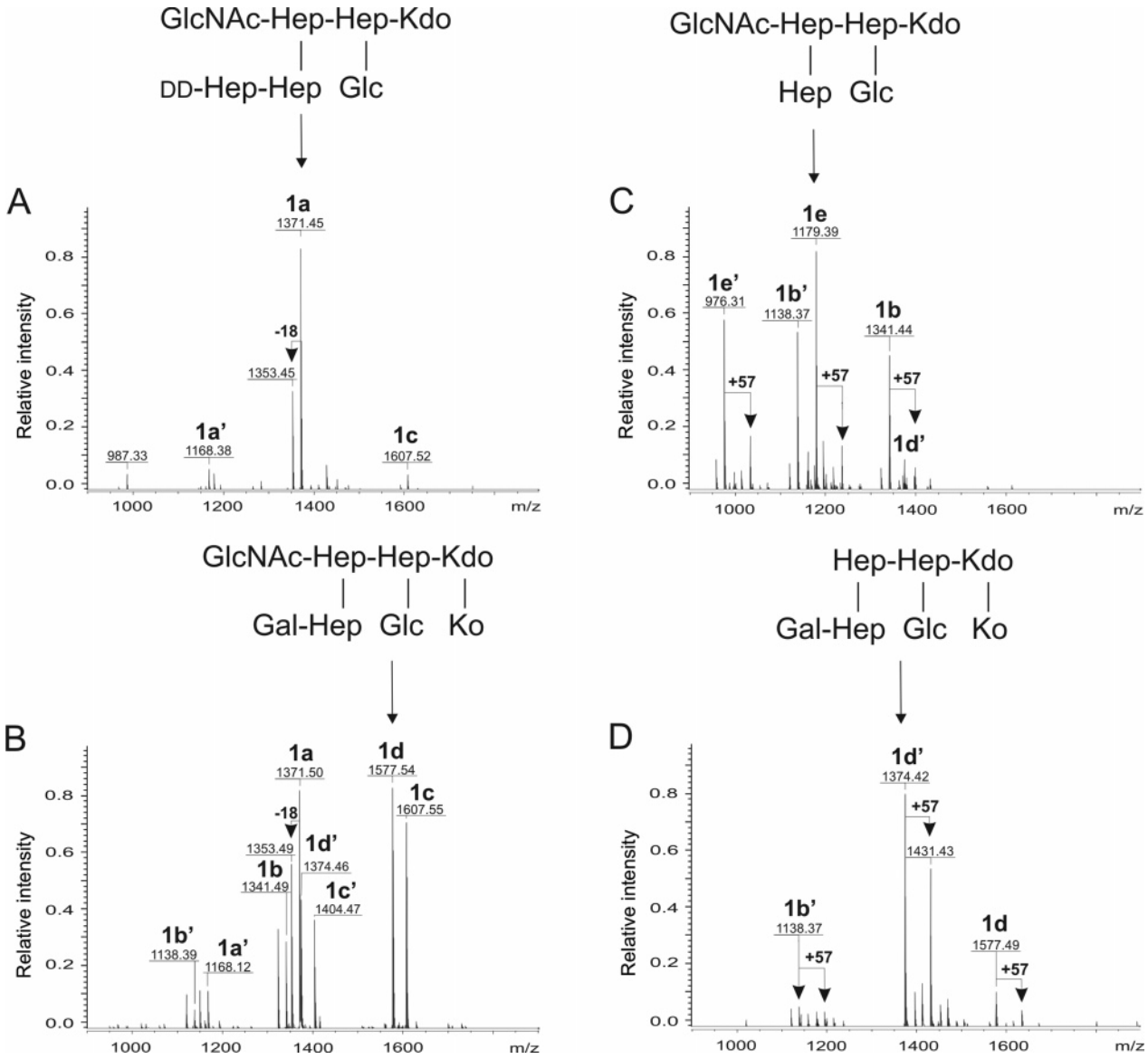

FIGURE 2: Charge deconvoluted negative ion ESI FT−ICR mass spectra of OS-37_{218} (A), OS-25_{218} (B), OS-37_{1146} (C), and OS-25_{1146} (D) and explanation of structural variants **1a**, **1d**, **1d′**, and **1e** (see text).

mass as in that of OS-37_{218} (Figure 2A), indicating the presence of the same heptasaccharide. Another peak indicated the presence of a related hexasaccharide that lacked GlcNAc (compound **1a′**), with a calculated degree of substitution of OS-25_{218} with GlcNAc being ~65%. Ions of another series in OS-25_{218} indicated the presence of a heptasaccharide, along with a hexasaccharide that was not found in OS-37_{218} and differed from compounds **1a** and **1a′** by −30 Da. This sturuture had a replacement of one of the heptose residues (DD-Hep, see below) with Gal. Thus, OS-25_{218} contains a heptasaccharide composed of $GlcNAc_1Glc_1Gal_1Hep_3Kdo_1$ (**1b**) and a hexasaccharide composed of $Glc_1Gal_1Hep_3Kdo_1$ (**1b′**). Two remaining ions were detected in OS-25_{218} that were characterized by a mass difference of +236 Da from ions **1a**, **1a′**, **1b** and **1b′**, evidently belonging to compounds with one additional Ko residue. They included peaks for two major octasaccharides $GlcNAc_1Glc_1Hep_4Kdo_1Ko_1$ (**1c**) and $GlcNAc_1Glc_1Gal_1Hep_3Kdo_1Ko_1$ (**1d**) with molecular masses 1607.6 and 1577.5 Da, and two minor GlcNAc-lacking heptasaccharides **1c′** and **1d′** (−203 Da), respectively.

Overall, these results indicate the occurrence of several LPS core oligosaccharide variants in *Y. pestis* ssp. *pestis* strain KM218, whose ratios vary significantly with growth temperature. Further determinations of the oligosaccharide structures from *Y. pestis* ssp. *pestis* were carried out on fractionated oligosaccharides OS-37_{218} and OS-25_{218} that were separated into differentially charged components by anion-exchange chromatography on a HiTrap Q column (Figure 3). OS-37_{218} had only one major acidic fraction, II, whereas OS-25_{218} yielded two acidic fractions, II and III, which corresponded to Ko-lacking and Ko-containing oligosaccharides, respectively. ESI FT−ICR MS showed that fraction II from OS-37_{218} contains mainly oligosaccharide **1a** with a molecular mass of 1371.45 Da (see Figure 2A), whereas fraction II from OS-25_{218} is a mixture of oligosaccharides **1a** and **1b** with molecular masses of 1371.50 and 1341.49 Da and fraction III is a mixture of oligosaccharides **1c** and **1d** with molecular masses of 1607.55 and 1577.54 Da, respectively (see Figure 2B). Each fraction also contained the smaller-sized oligosaccharide lacking GlcNAc.

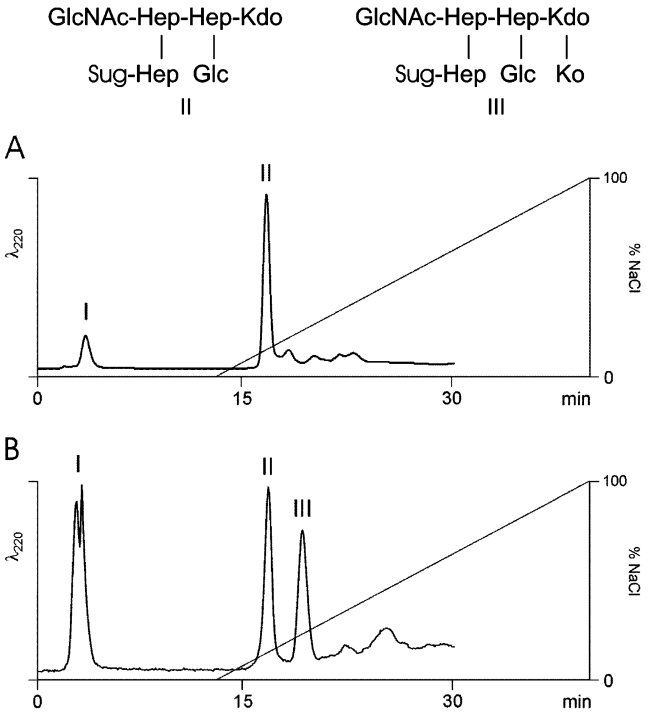

FIGURE 3: HiTrap Q anion-exchange chromatography profile of OS-37_{218} (A) and OS-25_{218} (B). Fractions II and III are explained on the top (Sug is DD-Hep in A or either DD-Hep or Gal in B); fraction I is a neutral contaminant.

Analysis of the Oligosaccharides from Y. pestis KM260-(11) and KIMD1. To determine if there was a significant structural variability in the LPS oligosaccharides among different biovar strains of *Y. pestis* ssp. *pestis*, we next analyzed the oligosaccharides isolated from strains KM260(11) (bv. orientalis) and KIMD1 (bv. antiqua). Essentially the same oligosaccharide structures were found in OS-37 and OS-25 from these strains (Table 3) as was found in those from *Y. pestis* KM218. Strains KM260(11) and KIMD1 differed by having a slightly higher content of the Ko-containing compound in OS-37, which was present in only small amounts in OS-37 from strain KM218. Overall, the LPS oligosaccharide structures determined for three different strains of *Y. pestis* ssp. *pestis* were highly similar.

Linkage Analysis and Full Elucidation of the Structure of the Oligosaccharides from the LPS of Y. pestis KM218. Methylation of fraction III (Figure 3) from OS-25_{218} followed by hydrolysis and analysis by GLC−MS of the derived alditol acetates revealed 2,6,7-tri-*O*-methyl, 2,4,6-tri-*O*-methyl, and 2,3,4,6-tetra-*O*-methyl derivatives of LD-Hep indicating these methylated sugars were derived from 3,4-disubstituted, 3,7-disubstituted and 7-substituted LD-Hep residues. Additionally present was the 2,3,4,6,7-penta-*O*-methyl derivative of DD-Hep, 2,3,4,6-tetra-*O*-methylgalactose, and 2-amino-2-deoxy-2,3,4,6-tetra-*N*,*O*-methylglucose. As these methylated sugars had all of the available hydroxyl groups methylated, they indicate the presence of DD-Hep, Gal, and GlcNAc as terminal residues.

Fraction III from OS-25_{218} was reduced with sodium borohydride and further fractionated by high-performance anion-exchange chromatography on CarboPac PA1 at super-high pH to give reduced oligosaccharides **1c** and **1d**. Their complete structures, as well as that of oligosaccharide **1a** contained in fraction II from OS-37_{218}, were established by one- and two-dimensional ^{1}H and ^{13}C NMR spectroscopy using methodology described previously (*15*, *30*) (for ^{1}H NMR spectra and signal assignment see Supporting Information). In addition, the ^{1}H NMR spectrum of a mixture of oligosaccharides **1a** and **1b** (fraction II from OS-25_{218}) was compared with the spectra of compounds **1a**, **1c**, and **1d**. As a result, it was found that oligosaccharides **1a** and **1c** differ from the related oligosaccharides **1b** and **1d** by replacement of a terminal D-α-D-Hep with a terminal β-Gal. Oligosaccharides **1a** and **1c** and oligosaccharides **1b** and **1d** differ from each other by the presence of a terminal α-Ko residue in compounds **1c** and **1d**. Therefore, the NMR data demonstrated that oligosaccharides isolated from the LPS of *Y. pestis* KM218 have the following structures:

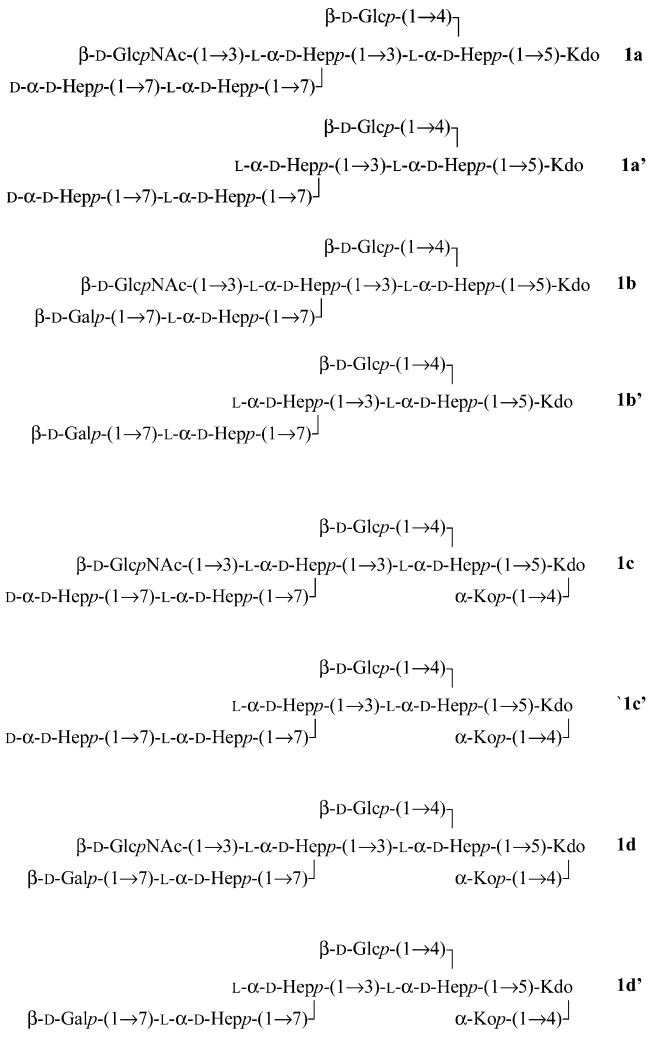

Oligosaccharides **1a** and **1b** were evidently derived from the LPS molecules containing the second, terminal Kdo residue, which was cleaved by mild acid hydrolysis. In contrast, when present, the terminal Ko residue was not hydrolyzed and, as a result, oligosaccharides **1c** and **1d** were obtained. The stability of the ketosidic linkage of Ko during methanolysis has been reported (*31*).

Structural analysis of the oligosaccharides from Y. pestis *ssp.* caucasica *strain 1146.* In accordance with the GLC analysis of the sugar components of OS-25_{1146} and OS-37_{1146} (Table 2), the ESI FT−ICR MS spectrum of these molecules (Figures 2C and 2D) showed the absence of DD-Hep from

Table 3: Molecular Mass (Da) and Occurrence of Various Core Variants **1** in OS-25 and OS-37 from Wild-Type-LPS *Y. pestis* Strains[a]

	variable core components				*Y. pestis* ssp. *pestis*						*Y. pestis* ssp. *caucasica*	
					KM218		KM260(11)		KIMD1		1146	
1	**D**	**J** or **K**	**H**	mol mass	OS-25	OS-37	OS-25	OS-37	OS-25	OS-37	OS-25	OS-37
a	H[b]	D-α-D-Hep	β-GlcNAc	1371.44	++	++	+	++	++	++		
b	H[b]	β-Gal	β-GlcNAc	1341.43	++		+		+			++
c	α-Ko	D-α-D-Hep	β-GlcNAc	1607.49	++	±	++	+	++	+		
d	α-Ko	β-Gal	β-GlcNAc	1577.48	++		++	±	++		+	
e	H[b]	H	β-GlcNAc	1179.38								++
a′	H[b]	D-α-D-Hep	H	1168.35	+	+	+	+	++	+		
b′	H[b]	β-Gal	H	1138.36	+		+		+		++	++
c′	α-Ko	D-α-D-Hep	H	1404.41	++		++		++			
d′	α-Ko	β-Gal	H	1374.40	++		++		++		++	+
e′	H[b]	H	H	976.30								++

[a] Given estimates are based on the ESI FT-ICR MS data. [b] Derived by cleavage of α-Ko during mild acid hydrolysis of the LPS. Key: ++, major; +, minor; ±, trace.

both (Table 3). The major compounds identified in OS-37_{1146} (Figure 2C) were heptasaccharide **1b** and a comparable amount of the related hexasaccharide lacking Gal (**1e**) as well as the corresponding GlcNAc-lacking compounds **1b′** and **1e′**. OS-25_{1146} included oligosaccharide **1d** as a minor product and the corresponding GlcNAc-lacking compound **1d′** as the main product (Figure 2D). Thus, in OS-25_{1146} Gal occurs as a terminal monosaccharide in all molecules but only in half the molecules in OS-37_{1146}. The oligosaccharide from *Y. pestis* 1146 synthesized at both 25 °C and 37°C are distinguished from those from the *Y. pestis* ssp. *pestis* strains by a lower content of GlcNAc. Additional minor peaks were found in the mass spectra for most of the compounds from *Y. pestis* 1146, which had molecular masses higher by 57 Da. This was attributed to substitution of the oligosaccharides with glycine (see below). The content of the glycine-substituted compounds was markedly higher in OS-25_{1146} as compared to OS-37_{1146}.

β-D-Glc*p*-(1→4)-┐
β-D-Glc*p*NAc-(1→3)-L-α-D-Hep*p*-(1→3)-L-α-D-Hep*p*-(1→5)-Kdo **1e**
L-α-D-Hep*p*-(1→7)-┘

β-D-Glc*p*-(1→4)-┐
L-α-D-Hep*p*-(1→3)-L-α-D-Hep*p*-(1→5)-Kdo **1e'**
L-α-D-Hep*p*-(1→7)-┘

On HiTrap Q anion-exchange chromatography, OS-37_{1146} and OS-25_{1146} eluted in essentially the same patterns as was observed for OS-37_{218} and OS-25_{218} from *Y. pestis* ssp. *pestis* strain KIM218 (see Figure 3), except for a lower overall amount of fraction II in OS-25_{1146} that contains Ko-lacking compounds. Fraction III from OS-25_{1146} and fraction II from OS-37_{1146} were studied by one- and two-dimensional NMR spectroscopy as described above. This analysis confirmed the data of the MS studies and, particularly, showed that, in addition to oligosaccharides **1b** and **1d**, an oligosaccharide, **1e**, lacking both Gal and DD-Hep was present. Overall, the major difference found in the oligosaccharides between the isolates of *Y. pestis* ssp. *pestis* and *Y. pestis* ssp. *caucasica* was the lack in the latter of oligosaccharides terminated with DD-Hep.

Structural Analysis of the Oligosaccharides from Y. pestis EV11M. The ESI FT−ICR mass spectra of OS-37_{11M} and OS-25_{11M} isolated from the LPS of the mutant strain *Y. pestis* EV11M demonstrated a mixture of Kdo−Kdo and Ko−Kdo disaccharides in both samples. OS-37_{11M} and OS-25_{11M} were fractionated by gel chromatography on TSK HW-40 to give two disaccharides from each preparation. The ^{1}H and ^{13}C NMR chemical shifts (see Supporting Information) and two-dimensional NMR spectroscopy data demonstrated that these are α-Kdo-(2→4)-Kdo and α-Ko-(2→4)-Kdo disaccharides, and that Kdo at the reducing end is present in a 2,7-anhydro form (see Supporting Information). The α-Ko-(2→4)-Kdo disaccharide has been isolated earlier from the LPS of *Burkholderia cepacia* (*31*) and the α-Kdo-(2→4)-Kdo disaccharide from the LPS of a Re mutant of *Salmonella enterica* (*32*).

Remarkably, as opposed to the oligosaccharides in the other *Y. pestis* ssp. *pestis* strains studied, the terminal Kdo residue in OS-25_{11M} and OS-37_{11M} was not cleaved upon mild acid degradation of the LPS, evidently due to the lack of the heptose substituent at position 5, which, when present, renders the ketosidic linkage acid-labile.

Structural Studies of Lipid A. Fatty acid composition and the overall structure of lipid A (Figure 4) from the *Y. pestis* strains cultivated at different temperatures were determined using GLC−MS analysis of the acetylated methyl esters and ESI FT−ICR MS of lipid A samples isolated by mild acid degradation of the LPS. In LA-37_{218} only 3-hydroxymyristic acid [14:0(3-OH)] was present. LA-25_{218} contained a major amount of 14:0(3-OH) and minor amounts of palmitoleic acid (16:1) and lauric acid (12:0). This finding is consistent with published data on *Y. pestis* lipid A composition (*22*, *23*). Palmitoleic acid in *Y. pestis* has been formerly identified as 16:1ω9cis (*33*). Both LA-37_{11M} and LA-25_{11M} from the mutant strain *Y. pestis* EV11M similarly contained mainly 14:0(3-OH) but were distinguished by the presence of a minor amount of palmitic acid (16:0).

The negative ion ESI FT−ICR mass spectrum of LA-37_{218} comprised two major peaks for compounds with molecular masses 1404.85 and 1178.66 Da, which corresponded to tetraacyl and triacyl lipid A species consisting of a bisphosphorylated glucosamine disaccharide backbone with four and three primary 14:0(3-OH) acyl groups attached. Furthermore, peaks for compounds carrying an additional Ara4N residue (+131 Da) were detected with lower intensity. LA-25_{218} contained the same major tetraacyl and minor triacyl species and, in addition, minor pentaacyl and hexaacyl species. Each

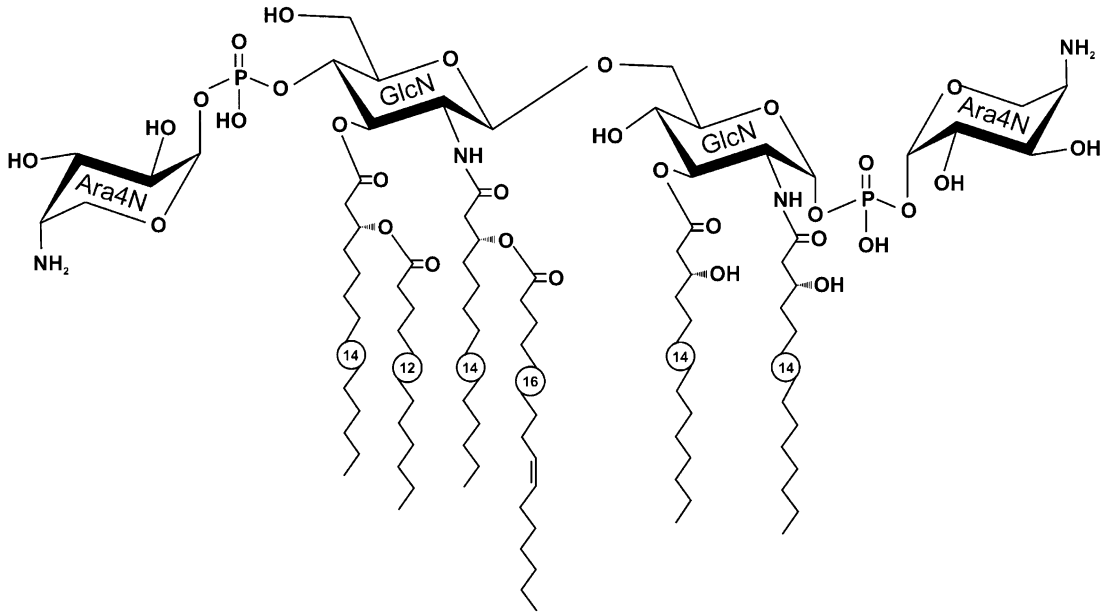

FIGURE 4: Structure of hexaacyl lipid A species with two Ara4N residues in LA-25 from *Y. pestis* KM218. The most abundant form of the LPS, the tetraacyl form, lacks the two secondary fatty acids (C12:0 and C16:1). The structure of the fatty acid 16:1 (*33*) and the position of the secondary fatty acids 12:0 and 16:1 (*22*) are shown based on published data.

species gave a series of ions for compounds with no, one and two Ara4N residues. As compared with the tetraacyl species, the pentaacyl species included an additional 12:0 acyl group (mass difference 182 Da) and the hexaacyl species two additional fatty acids, 12:0 and 16:1 (mass difference 182 + 236 = 418 Da), all being evidently attached as secondary acyl groups. A hexaacyl species with the same composition and, most likely, the same structure (Figure 4) has been reported as the major component in lipid A from *Y. pestis* EV40 grown at 28 °C (*22*).

Structural Studies of the Whole LPS from Y. pestis KM218, KM260(11), and KIMD1. The data derived from the study of the isolated oligosaccharide and lipid A components of the LPS from the *Y. pestis* ssp. *pestis* strains was used to determine the structure of the intact LPS molecule using negative ion ESI FT−ICR mass spectroscopy. In LPS-37_{218} the largest peak was from compound **3a** (Figure 5A) with molecular mass 3240.51 Da, which corresponded to an LPS species having tetraacyl lipid A with two Ara4N residues and the DD-Hep- and Kdo-containing oligosaccharide, which corresponded to oligosaccharide **1a** but with an additional terminal Kdo residue. No peaks for higher acylated species were present. Two other major peaks corresponded to compounds lacking one and two Ara4N residues. There were also ions corresponding to the minor structures **3b** and **3d** (Figure 5A) wherein Gal substituted for DD-Hep and Ko substituted for Kdo. Another minor series of ions identified in the mass spectra of LPS-37_{218} were those from compounds with molecular masses higher by 57 Da, and this was attributed to Gly containing species. The identity of glycine was confirmed by amino acid analysis after full acid hydrolysis of the LPS. A capillary skimmer dissociation (CSD) experiment with the whole LPS revealed a pair of Y,B-fragment ions corresponding to the lipid A and core moieties, respectively, confirming that glycine is a component of the core (data not shown). The exact location of glycine in the core was not determined.

As one major immune mechanism possessed by invertebrates and mammals alike is production of anti-microbial peptides, we further investigated the effect of growth of *Y. pestis* in the presence of polymyxin B on the LPS structure. Cultivation of strain KM218 at 37 °C in the presence of polymyxin B resulted in a significant increase in the content of Ara4N and to some extent of glycine (compare the relative intensities of the mass peaks for Ara4N- and glycine-containing ions in Figures 5B and 5A), suggesting a role for these substituents in resistance to antimicrobial peptides.

Growing *Y. pestis* KM218 at 25 °C resulted in more LPS molecules with increased acylation. In addition to the tetraacyl LPS species that predominated in LPS-37_{218}, the LPS-25_{218} included pentaacyl and hexaacyl species (Figure 5C). The three different acylation patterns were associated with all possible oligosaccharide glycoforms to give compounds from **3a** through **3d**, the Gal- & Kdo-containing compound **3b** being minor (Figure 5C). Interestingly, while the secondary fatty acid 12:0 is distributed almost uniformly between the molecules with different oligosaccharide glycoforms, 16:1 is preferentially associated with Ko-containing glycoforms **1c** and **1d**. Only small amounts of Ara4N-lacking compounds were present, and hence, in LPS-25_{218} the content of Ara4N is close to stoichiometric.

No peaks corresponding to LPS with a triacyl lipid A moiety were observed in the mass spectra of the whole LPS-25_{218} and LPS-37_{218}, thus indicating that those observed in the isolated lipid A (see above) were artifacts due to partial O-deacylation in the course of mild acid degradation of the LPS. The ESI MS data of the whole LPS confirmed that Kdo-lacking oligosaccharides **1a** and **1b** are not present in the intact LPS, likely occurring in the oligosaccharides as a result of cleavage of the terminal Kdo residue during mild acid hydrolysis.

LPS-37 and LPS-25 from *Y. pestis* KM260(11) and KIMD1 showed essentially the same MS pattern with respect to intact LPS structure except that when grown at 37 °C, *Y. pestis* KIMD1 produced a minor amount of pentaacyl LPS

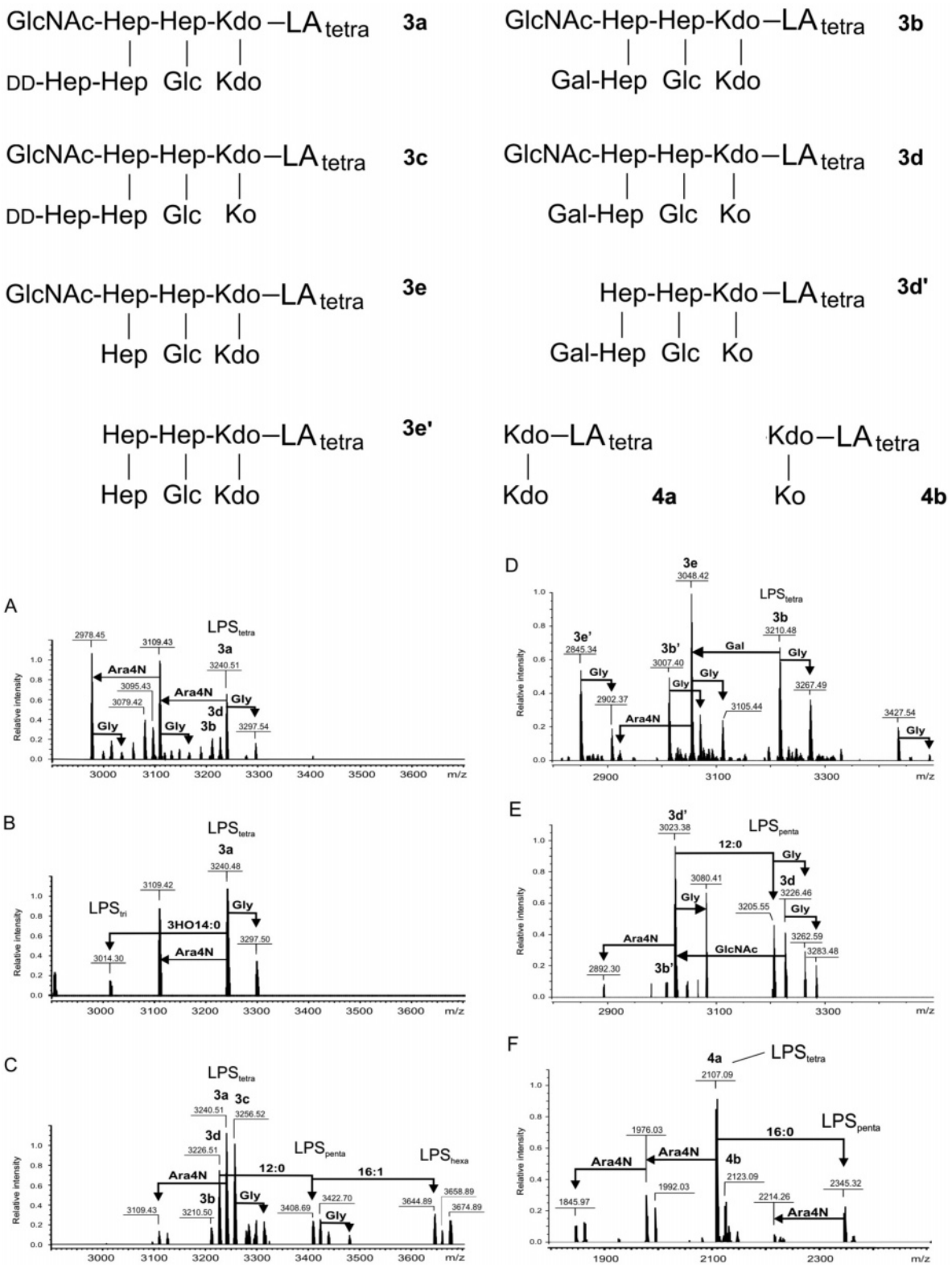

FIGURE 5: Charge deconvoluted negative ion ESI FT−ICR mass spectra of LPS-37_{218} (A), LPS-37_{218}−PMB (B), LPS-25_{218} (C), LPS-37_{1146} (D), LPS-25_{1146} (E) and LPS-37_{11M} (F) and explanation of the LPS structural variants **3**. LPS_{tetra} stands for tetraacyl species etc.

species rather than solely a tetraacyl LPS species (Table 4).

Structural Studies of the Whole LPS from Y. pestis ssp. caucasica 1146. Again, ESI FT−ICR mass spectrometry was used to study the structure of the intact LPS of *Y. pestis* 1146. LPS-37_{1146} showed only tetraacyl lipid A species containing two Ara4N residues (Figure 5D). The major peaks were for compound **3b** containing the oligosaccharide glycoform **1b,** and compound **3e** with the Gal-lacking glycoform **1e,** as well as the corresponding compounds **3b′** and **3e′** lacking GlcNAc and some molecules that were substituted with Gly. LPS-25_{1146} was distinguished by the presence of additional pentaacyl lipid A species, again with most of the molecules containing two Ara4N residues (Figure 5E). The major compounds in LPS-25_{1146} were **3d** with the Gal- & Ko-containing core glycoform **1d** and the corresponding compound **3d′** containing oligosaccharide **1d′** lacking GlcNAc.

Table 4: Occurrence of Lipid A Variants in the LPS of Various *Y. pestis* Strains[a]

	Y. pestis ssp. *pestis*						*Y. pestis* ssp. *caucasica*		*Y. pestis* mutant	
	KM218		KM260(11)		KIMD1		1146		EV11M	
lipid A type	LPS-25	LPS-37	LPS-25	LPS-37	LPS-25	LPS-37	LPS-25	LPS-37	LPS-25	LPS-37
O-Acylation pattern										
tetraacyl species [4 × 14:0(3-OH)]	++	++	++	++	++	++	++	++	++	++
pentaacyl species (tetraacyl + 12:0)	+	±	+		+	+	++		+	+
hexaacyl species (tetraacyl + 12:0 + 16:1)	+		±		+					
no. of Ara4N residues										
two	++	++	++	++	++	+	++	++	++	++
one	+	++	+	++	+	++	±	±	++	+
no		++		+		++			+	+

[a] Given estimates are based on the ESI FT-ICR MS data of the whole LPS. ++, major; +, minor; ±, trace.

The content of Gly containing species was markedly higher in LPS-25_{1146} as compared to LPS-37_{1146}.

Structural Studies of the whole LPS from Y. pestis ssp. pestis mutant strain EV11M. The ESI FT−ICR mass spectra of LPS-37_{11M} (Figure 5F) and LPS-25_{11M} were similar to each other. The major species detected were the tetraacyl LPS species with two Ara4N residues attached to either Kdo−Kdo or Ko−Kdo disaccharide core having molecular masses 2107.09 and 2123.09 Da (Figure 5, compounds **4a** and **4b**, respectively). Ara4N is present in nonstoichiometric amounts in both LPS preparations and its content is higher in LPS-37_{11M}. The mass spectra confirmed the occurrence of the fatty acid 16:0, which is evidently attached as a secondary acyl group at an undetermined position to form a minor pentaacyl lipid A species in both LPS-37_{11M} and LPS-25_{11M}. Overall, the data obtained show that ESI FT−ICR MS of the whole LPS is a useful tool for analysis of the structural diversity in the LPS of *Y. pestis*.

DISCUSSION

The LPS of most Gram-negative bacteria plays multiple important roles in pathogenesis, epidemiology and disease control. The structures of the LPS components, such as the O side chain, the core oligosaccharide linked to the lipid A backbone, and the lipid A itself, all affect the organism's virulence. In addition, these structures can determine recognition of a pathogen by the innate and acquired host immune system, identification by serologic classification, and even can be a target for protective immunity. Thus, basic knowledge of the overall structure of the LPS of pathogenic Gram-negative bacteria can provide significant insight into numerous aspects of virulence, particularly when structures of related strains with greater and lesser virulence can be compared.

In the case of *Y. pestis*, the majority of the studies carried out on this organism have focused on the genetically homogeneous strains of bv. orientalis primarily found in North and South America, whose pauciclonality can be attributed to the lack of plague in the Americas prior to the introduction of *Y. pestis* by infected rats carried to the port of San Francisco from Hong Kong in 1902. The introduced strain has apparently spread throughout the Americas, where it is now found essentially in sylvatic foci, and there does not appear to have been much genetic change in American isolates over the last 100 years (*4*). Yet in European Russia and in Asia there is a great diversity of *Y. pestis* strains, many of which can be classified into different subspecies based on a variety of characteristics (*4*). The potential for virulence in humans of these non-American strains, and their potential as agents of bioterrorism, has to be considered because such strains could be used to avoid detection by reagents with specificity to structures such as LPS oligosaccharides and lipid A, and could also avoid immunologic control elicited by active and passive vaccination (*4*). In addition, because *Y. pestis* is introduced into mammals by fleas with generally lower, exothermically determined temperatures, structural variations in key surface molecules that are dependent on growth temperature could also impact the detection and control efforts for plague. Thus, full knowledge of the variation in attributes of these non-American *Y. pestis* strains, including structural variation in the LPS, is essential for proper preparedness in identifying and reacting to human infection with *Y. pestis*.

The data obtained here regarding the variation in the LPS structure in strains of *Y. pestis* found in Eurasia and Madagascar and a mutant strain previously known to have uncharacterized changes in its LPS clearly demonstrate that in wild-type-LPS strains of *Y. pestis* the oligosaccharide structure is affected by the growth temperature. At 37 °C, the glycoform that is mainly expressed by *Y. pestis* ssp. *pestis* has terminal Kdo and DD-Hep residues, whereas at 25 °C, four glycoforms that adopt all possible combinations of four terminal glycosyl groups (Kdo/Ko and DD-Hep/Gal) are present. Therefore, there are two types of variations in the core oligosaccharide structure: in one variation, a terminal DD-Hep residue interchanges with a Gal residue, and in another variation, a terminal Kdo residue is variably substituted with a Ko residue.

Among *Yersinia* species, the Gal-containing glycoforms are unique to *Y. pestis*, whereas a similar DD-Hep-containing glycoform occurs in *Y. enterocolitica* (*34*) and replacement of Kdo with Ko has been reported in the core of some other bacteria, e.g. in *Burkholderia cenocepacia* (*31*). The LPS of *Y. pestis* ssp. *caucasica* differed somewhat from *Y. pestis* ssp. *pestis* by the absence of DD-Hep in any of the oligosaccharide glycoforms, but, as in the other wild-type-LPS *Y. pestis* strains studied, the content of galactose decreased markedly with an increase in the growth temperature, and the alternations in the amount of Kdo and Ko also showed the same temperature dependence. As *Y. pestis* ssp. *caucasica* is known to have reduced virulence for guinea pigs (*4*) and is not a significant cause of human infection, it may be that the differences in its LPS structure limit the

virulence to a restricted range of mammalian hosts, mainly voles and mice.

Other studies shed further light on the genetic basis for changing the LPS structure of *Y. pestis*. For example, a *phoP* mutant of *Y. pestis* strain GB grown at 28 °C contains DD-Hep but lacks Gal, indicating that synthesis of parts of the LPS oligosaccharide are regulated by the PhoP/PhoQ two-component signal transduction system (*11*). Therefore, mutation in the *phoP* gene (*11*) caused the same alteration in the core structure as did elevation of growth temperature, as demonstrated in this work. This finding suggests that when the temperature decreases, the PhoP/PhoQ system directs the LPS oligosaccharide biosynthesis toward the Gal-containing glycoforms.

In *Y. pestis* ssp. *pestis*, 10−35% of the oligosaccharides can lack the terminal GlcNAc residue, and *Y. pestis* ssp. *caucasica* is distinguished by even a lower content of GlcNAc in the LPS. However, it is not clear if GlcNAc is truly a component of the *Y. pestis* core oligosaccharide or is related to the fact that the *Y. pestis* LPS lacks O-antigen, and the GlcNAc residue represents what would be the first, and thus acceptor, sugar for the missing O antigen. This conclusion is consistent with the finding of the attachment of a single β-GlcNAc residue to the LPS core in an O-antigen-deficient mutant of *Y. enterocolitica* O8 (*34*) although there was no GlcNAc in the LPS of a wild-type-LPS strain of *Y. enterocolitica* O9 (*35*). *Y. pestis* does not completely lack the O-antigen gene cluster but has a faulty one closely related to the *Yersinia pseudotuberculosis* serotype O1b gene cluster (*13, 36*), from which *Y. pestis* has likely evolved (*14, 37*). Comparison of the nucleotide sequences in the O-antigen gene clusters of *Y. pseudotuberculosis* O1b and *Y. pestis* showed almost 100% identity between all genes, except for the *wzx* genes for an O-unit transporter (flippase) present in the *wzy*-dependent O-antigen pathway (*38*), which were only 90.4% identical (*14*). It has been shown that flippase in *E. coli* can incorporate GlcNAc onto the LPS core (*39*). The flippase in *Y. pestis* may thus be able to translocate undecaprenyl diphosphate-linked GlcNAc onto the LPS core oligosaccharide in the absence of an O-antigen unit.

The lipid A structure of *Y. pestis* also significantly varies depending on growth temperature. Although tetraacyl lipid A species are most abundant at both temperatures studied, at 25 °C additional pentaacyl and hexaacyl species are produced. Furthermore, in *Y. pestis* ssp. *pestis* the degree of glycosylation of phosphate groups in lipid A with Ara4N is significantly higher and is nearly stoichiometric at 25 °C compared with that at 37 °C. A similar temperature dependence of the lipid A structure has been reported for some other *Y. pestis* strains (*23, 40*), and it was found that the *Y. pestis phoP* gene is required for Ara4N modification but not for the temperature-dependent changes in acylation (*40*).

In addition, we found that changes in the lipid A structure could be induced not only by changes in growth temperature but also by including polymyxin B in the growth medium, which caused a significant increase in the content of Ara4N in *Y. pestis* ssp. *pestis* KM218 cultivated at 37 °C. These structural variations may have important implications for the pathogenesis of *Y. pestis* infection. The introduction of *Y. pestis* from cooler fleas into mammalian skin is followed by formation of the inflammatory swelling of the regional lymph nodes (i.e., bubonic plague), which is likely dependent on the host response to the lipid A via interactions with toll-like receptors on macrophage-like cells in the skin and lymph nodes. Changes in lipid A following growth at mammalian temperatures could also be important in the pathogenesis of the transmissible form of pneumonic plague. Knowledge of the structural variation provided here will be key to understanding different host responses to *Y. pestis* LPS that vary with growth temperature of the organism and may underlie the different disease manifestations that occur with *Y. pestis* infection.

In *Y. pestis* ssp. *caucasica* the growth temperature had no significant influence on the substitution of lipid A with Ara4N, which was nearly stoichiometric in all samples analyzed. A structural component of the LPS of this strain was an amino acid, glycine, present on some of the oligosaccharide molecules at a currently undetermined location.

In the deep-rough mutant *Y. pestis* EV11M, the LPS oligosaccharide is a disaccharide linked to a tetraacyl or pentaacyl lipid A species. The latter has a secondary fatty acid (16:0) that is different from those in wild-type-LPS strains (12:0 and 16:1). The mutation(s) in strain EV11M resulted not only in the loss of a large part of the LPS oligosaccharide and the change in fatty acid composition but also affected the system that determines the degree of lipid A acylation, which is essentially the same at both temperatures studied, although the content of Ara4N is higher at 37 °C rather than at 25 °C. We do not know if the changes in lipid A acylation in the EV11M mutant strain are secondary to the changes in the core oligosaccharide or represent independent genetic events, but the ability of *Y. pestis* to be viable with the determined structural variation in the lipid A could also represent a means to manipulate these strains and alter their virulence.

There are numerous ways in which the temperature-dependent and intraspecific variations in the *Y. pestis* LPS structure could have a biological significance. The production at 37 °C of a lower acylated LPS likely results in a less immunostimulatory LPS, which may compromise the host's ability to rapidly respond with a regulated and proper inflammatory response to infection (*23, 40*). Such a strategy could possibly promote the virulence and person-to-person spread of pneumonic plague. The content of 4-amino-4-deoxyarabinose in lipid A, which is higher at 25 °C and increases when bacteria are grown in the presence of polymyxin B, correlates with polymyxin B resistance of *Y. pestis* (ref. *23* and authors' unpublished data). This example could indicate an adaptive response of *Y. pestis* to growth in fleas, which elaborate anti-microbial peptides as a significant component of their innate immune systems. The latter finding is in agreement with a high sensitivity of a Gal-lacking *phoP* mutant of *Y. pestis* to polymyxin B when grown at 28 °C (*11*).

Overall, the findings of significant temperature-dependent variations in the LPS structure of the Eurasian/African strains of *Y. pestis* representing two different subspecies is likely a key feature of enzootic and epizootic pathogenesis of this organism. Furthermore, with the bioterrorism threat presented by this organism, understanding the natural diversity in structure and function of pathogenic factors like LPS, particularly among strains not found in the Americas, will

be essential for comprehensive preparedness for dealing with this threat.

ACKNOWLEDGMENT

We thank Dr. I. A. Dunaitsev (Obolensk, Russia) for large scale production of the *Y. pestis* biomasses, Dr. V. V. Amel'chenko (Obolensk, Russia) for drying of the biomasses and the LPS, and Mrs. A. N. Kondakova (Moscow, Russia) for assistance with ESI FT−ICR MS.

SUPPORTING INFORMATION AVAILABLE

Figures showing part of an electron impact mass spectrum of the Ko−Kdo disaccharide derivative and figures showing structures and ^{1}H NMR spectra and tables of ^{1}H and ^{13}C NMR data of core oligosaccharides from the lipopolysaccharide of *Yersinia pestis* ssp. *pestis* KM218. This material is available free of charge via the Internet at http://pubs.acs.org.

REFERENCES

1. Anisimov, A. P. (1999) [Factors providing for the blocking activity of *Yersinia pestis*: state of the art and prospects of research] [article in Russian], *Mol. Gen. Mikrobiol. Virusol.* (*4*), 11−15 [English translation: *Mol. Gen. Microbiol. Virol.* (*5*), 56−67].
2. Anisimov, A. P. (2002) [*Yersinia pestis* factors providing for circulation and persistence of the plague pathogen in ecosystems of natural foci. Communication 2] [article in Russian], *Mol. Gen. Mikrobiol. Virusol.* (*4*), 3−11 [English translation: *Mol. Gen. Microbiol. Virol.* (*5*), 1−14].
3. Anisimov, A. P. (2002) [*Yersinia pestis* factors ensuring circulation and persistence of the plague pathogen in ecosystems of natural foci. Communication 1] [article in Russian], *Mol. Gen. Mikrobiol. Virusol.* (*3*), 3−23 [English translation: *Mol. Gen. Microbiol. Virol.* (*4*), 1−30].
4. Anisimov, A. P., Lindler, L. E., and Pier, G. B. (2004) Intraspecific diversity of *Yersinia pestis*, *Clin. Microbiol. Rev. 17*, 434−464.
5. Brubaker, R. R. (2000) *Yersinia pestis* and bubonic plague, in *The prokaryotes, an evolving electronic resource for the microbiological community* (Dworkin, M., Falkow, S., Rosenberg, E., Schleifer, K.-H., Stackelbrandt, E., Eds.) Springer-Verlag, New York [On line] http://www.prokaryotes.com.
6. Domaradskii, I. V. (1993) *Plague: contemporary state, assumptions, problems.* Saratov Medical Institute Press, Saratov, Russia.
7. Perry, R. D., Fetherston, J. D. (1997) *Yersinia pestis* − etiologic agent of plague, *Clin. Microbiol. Rev. 10*, 35−66.
8. Parkhill, J., Wren, B. W., Thomson, N. R., Titball, R. W., Holden, M. T., Prentice, M. B., Sebaihia, M., James, K. D., Churcher, C., Mungall, K. L., Baker, S., Basham, D., Bentley, S. D., Brooks, K., Cerdeno-Tarraga, A. M., Chillingworth, T., Cronin, A., Davies, R. M., Davis, P., Dougan, G., Feltwell, T., Hamlin, N., Holroyd, S., Jagels, K., Karlyshev, A. V., Leather, S., Moule, S., Oyston, P. C., Quail, M., Rutherford, K., Simmonds, M., Skelton, J., Stevens, K., Whitehead, S., and Barrell, B. G. (2001) Genome sequence of *Yersinia pestis*, the causative agent of plague, *Nature 413*, 523−527.
9. Perry, R. D. (2003) A plague of fleas − survival and transmission of *Yersinia pestis*, *ASM News 69*, 336−340.
10. Chart, H., Cheasty, T., and Rowe, B. (1995) Differentiation of *Yersinia pestis* and *Y. pseudotuberculosis* by SDS−PAGE analysis of lipopolysaccharide, *Lett. Appl. Microbiol. 20*, 369−370.
11. Hitchen, P. G., Prior, J. L., Oyston, P. C., Panico, M., Wren, B. W., Titball, R. W., Morris, H. R., and Dell, A. (2002) Structural characterization of lipo-oligosaccharide (LOS) from *Yersinia pestis*: regulation of LOS structure by the PhoPQ system, *Mol. Microbiol. 44*, 1637−1650.
12. Prior, J. L., Hitchen, P. G., Williamson, E. D., Reason, A. J., Morris, H. R., Dell, A., Wren, B. W., and Titball, R. W. (2001) Characterization of the lipopolysaccharide of *Yersinia pestis*, *Microb. Pathog. 30*, 49−57.
13. Prior, J. L., Parkhill, J., Hitchen, P. G., Mungall, K. L., Stevens, K., Morris, H. R., Reason, A. J., Oyston, P. C. F., Dell, A., Wren, B. W., and Titball, R. W. (2001) The failure of different strains of *Yersinia pestis* to produce lipopolysaccharide O-antigen under different growth conditions is due to mutations in the O-antigen gene cluster, *FEMS Microbiol. Rev. 197*, 229−233.
14. Skurnik, M., Peippo, A., and Ervelä, E. (2000) Characterization of the O-antigen gene clusters of *Yersinia pseudotuberculosis* and the cryptic O-antigen gene cluster of *Yersinia pestis* shows that the plague bacillus is most closely related to and has evolved from *Y. pseudotuberculosis* serotype O:1b, *Mol. Microbiol. 37*, 316−330.
15. Vinogradov, E. V., Lindner, B., Kocharova, N. A., Senchenkova, S. N., Shashkov, A. S., Knirel, Y. A., Holst, O., Gremyakova, T. A., Shaikhutdinova, R. Z., and Anisimov, A. P. (2002) The core structure of the lipopolysaccharide from the causative agent of plague, *Yersinia pestis*, *Carbohydr. Res. 337*, 775−777.
16. Porat, R., McCabe, W. R., and Brubaker, R. R. (1995) Lipopolysaccharide-associated resistance to killing of yersiniae by complement, *J. Endotoxin Res. 2*, 91−97.
17. Bengoechea, J.-A., Lindner, B., Seydel, U., Díaz, R., and Moriyón, I. (1998) *Yersinia pseudotuberculosis* and *Yersinia pestis* are more resistant to bactericidal cationic peptides than *Yersinia enterocolitica*, *Microbiology 144*, 1509−1515.
18. Brubaker, R. R. (2003) Interleukin-10 and inhibition of innate immunity to *Yersiniae*: roles of Yops and LcrV (V antigen), *Infect. Immun. 71*, 3673−3681.
19. Nedialkov, Y. A., Motin, V. L., and Brubaker, R. R. (1997) Resistance to lipopolysaccharide mediated by the *Yersinia pestis* V antigen-polyhistidine fusion peptide: amplification of interleukin-10, *Infect. Immun. 65*, 1196−1203.
20. Dmitrovskii, V. G. (1994) Toxic component of pathogenesis of plague infectious process: infective toxic shock, in *Prophylaxis and means of prevention of plague. Proceedings of the International scientific Conference dedicated to the centenary of discovery of the plague pathogen* (Stepanov, V. M., Ed.) pp 15−16, Scientific-Manufacturing Association of the Plague-Control Establishments, Almaty, Kazakhstan.
21. Dimopoulos, G. (2003) Insect immunity and its implication in mosquito-malaria interactions, *Cell. Microbiol. 5*, 3−14.
22. Aussel, L., Thérisod, H., Karibian, D., Perry, M. B., Bruneteau, M., and Caroff, M. (2000) Novel variation of lipid A structures in strains of different *Yersinia* species, *FEBS Lett. 465*, 87−92.
23. Kawahara, K., Tsukano, H., Watanabe, H., Lindner, B., and Matsuura, M. (2002) Modification of the structure and activity of lipid A in *Yersinia pestis* lipopolysaccharide by growth temperature, *Infect. Immun. 70*, 4092−4098.
24. Gremyakova, T. A., Vinogradov, E. V., Lindner, B., Kocharova, N. A., Senchenkova, S. N., Shashkov, A. S., Knirel, Y. A., Holst, O., Shaikhutdinova, R. Z., and Anisimov, A. P. (2003) The core structure of the lipopolysaccharide of *Yersinia pestis* strain KM218. Influence of growth temperature, *Adv. Exp. Med. Biol. 529*, 229−231.
25. Galanos, C., Lüderitz, O., and Westphal, O. (1969) A new method for the extraction of R lipopolysaccharides, *Eur. J. Biochem. 9*, 245−249.
26. Sawardeker, J. S., Sloneker, J. H., and Jeanes, A. (1965) Quantitative determination of monosaccharides as their alditol acetates by gas liquid chromatography, *Anal. Chem. 37*, 1602−1603.
27. Hakomori, S.-I. (1964) A rapid permethylation of glycolipids and polysaccharides catalyzed by methylsulfinyl carbanion in dimethyl sulfoxide, *J. Biochem.* (*Tokyo*) *55*, 205−208.
28. Kjaer, M., Andersen, K. V., and Poulsen, F. M. (1994) Automated and semiautomated analysis of homo- and heteronuclear multidimensional nuclear magnetic resonance spectra of proteins: the program PRONTO, *Methods Enzymol. 239*, 288−308.
29. Lönngren, J., and Svensson, S. (1974) Mass spectrometry in structural analysis of natural carbohydrates, *Adv. Carbohydr. Chem. Biochem. 29*, 41−106.
30. Duus, J. O., Gotfredsen, C. H., and Bock, K. (2000) Carbohydrate structural determination by NMR spectroscopy: Modern methods and limitations, *Chem. Rev. 100*, 4589−4614.
31. Isshiki, Y., Kawahara, K., and Zähringer, U. (1998) Isolation and characterisation of disodium (4-amino-4-deoxy-β-L-arabinofuranosyl)−(1→8)−(D-*glycero*-α-D-*talo*-oct-2-ulopyranosylonate)−(2→4)−(methyl 3-deoxy-D-*manno*-oct-2-ulopyranosid)onate from the lipopolysaccharide of *Burkholderia cepacia*, *Carbohydr. Res. 313*, 21−27.
32. Brade, H., Zähringer, U., Rietschel, E. T., Christian, R., Schulz, G., and Unger, F. M. (1984) Spectroscopic analysis of a 3-deoxy-D-*manno*-2-octulosonic acid (KDO)-disaccharide from the li-

popolysaccharide of a *Salmonella godesberg* Re mutant, *Carbohydr. Res. 134*, 157−166.
33. Leclercq, A., Guiyoule, A., El Lioui, M., Carniel, E., and Decallonne, J. (2000) High homogeneity of the *Yersinia pestis* fatty acid composition, *J. Clin. Microbiol. 38*, 1545−1551.
34. Oertelt, C., Lindner, B., Skurnik, M., and Holst, O. (2001) Isolation and structural characterization of an R-form lipopolysaccharide from *Yersinia enterocolitica* serotype O:8, *Eur. J. Biochem. 268*, 554−564.
35. Müller-Loennies, S., Rund, S., Ervela, E., Skurnik, M., and Holst, O. (1999) The structure of the carbohydrate backbone of the core-lipid A region of the lipopolysaccharide from a clinical isolate of *Yersinia enterocolitica* 0:9, *Eur. J. Biochem. 261*, 19−24.
36. Skurnik, M. (1999) Molecular genetics of *Yersinia* lipopolysaccharide, in *Genetics of Bacterial Polysaccharides* (Goldberg, J. B., Ed.) pp 23−51, CRC Press, Boca Raton, FL, New York, and Washington, DC.
37. Achtman, M., Zurth, K., Morelli, G., Torrea, G., Guiyoule, A., and Carniel, E. (1999) *Yersinia pestis*, the cause of plague, is a recently emerged clone of *Yersinia pseudotuberculosis*, *Proc. Natl. Acad. Sci. U.S.A.* 96, 14043−14048 [published erratum (2000) *Proc. Natl. Acad. Sci. U.S.A. 97*, 8192].
38. Raetz, C. R. H., and Whitfield, C. (2002) Lipopolysaccharide endotoxins, *Annu. Rev. Biochem. 71*, 635−700.
39. Feldman, M. F., Marolda, C. L., Monteiro, M. A., Perry, M. B., Parodi, A. J., and Valvano, M. A. (1999) The activity of a putative polyisoprenol-linked sugar translocase (Wzx) involved in *Escherichia coli* O antigen assembly is independent of the chemical structure of the O repeat, *J. Biol. Chem. 274*, 35129−35138.
40. Rebeil, R., Ernst, R. K., Gowen, B. B., Miller, S. I., and Hinnebush, B. J. (2004) Variation in lipid A structure in the pathogenic yersiniae, *Mol. Microbiol. 52*, 1363−1373.

BI048430F

Part of an electron impact mass spectrum of the Ko-Kdo disaccharide derivative obtained by methanolysis of the lipopolysaccharide of *Yersinia pestis* ssp. *pestis* KM218 LPS followed by acetylation. Explanation of the diagnostic ions is shown in the inset.

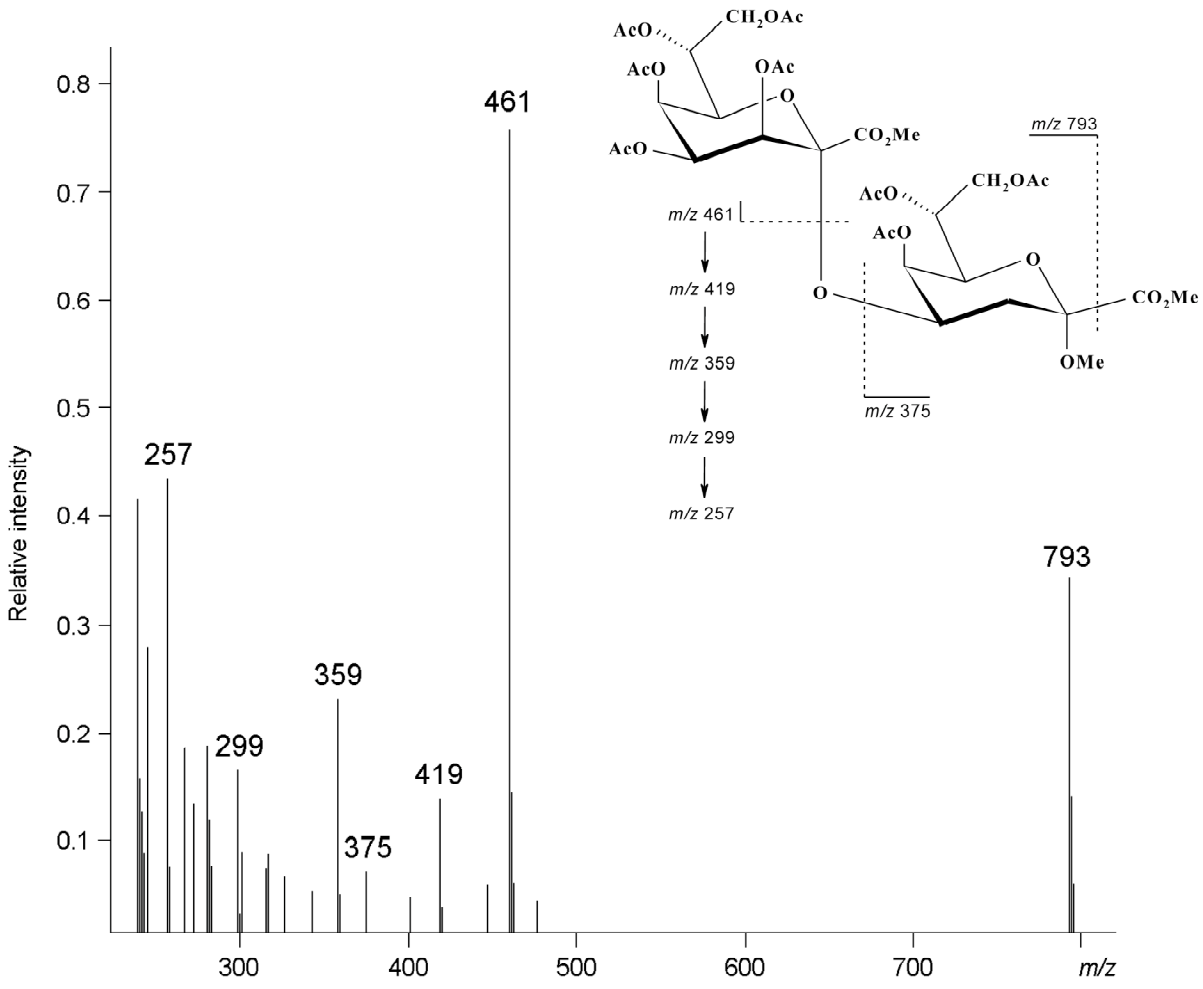

Structures, ^{1}H NMR spectra, and ^{1}H and ^{13}C NMR data of core oligosaccharides from the lipopolysaccharide of *Yersinia pestis* ssp. *pestis* KM218 cultivated at 37°C (**1a**) and 25°_ (**1c** and **1d**)

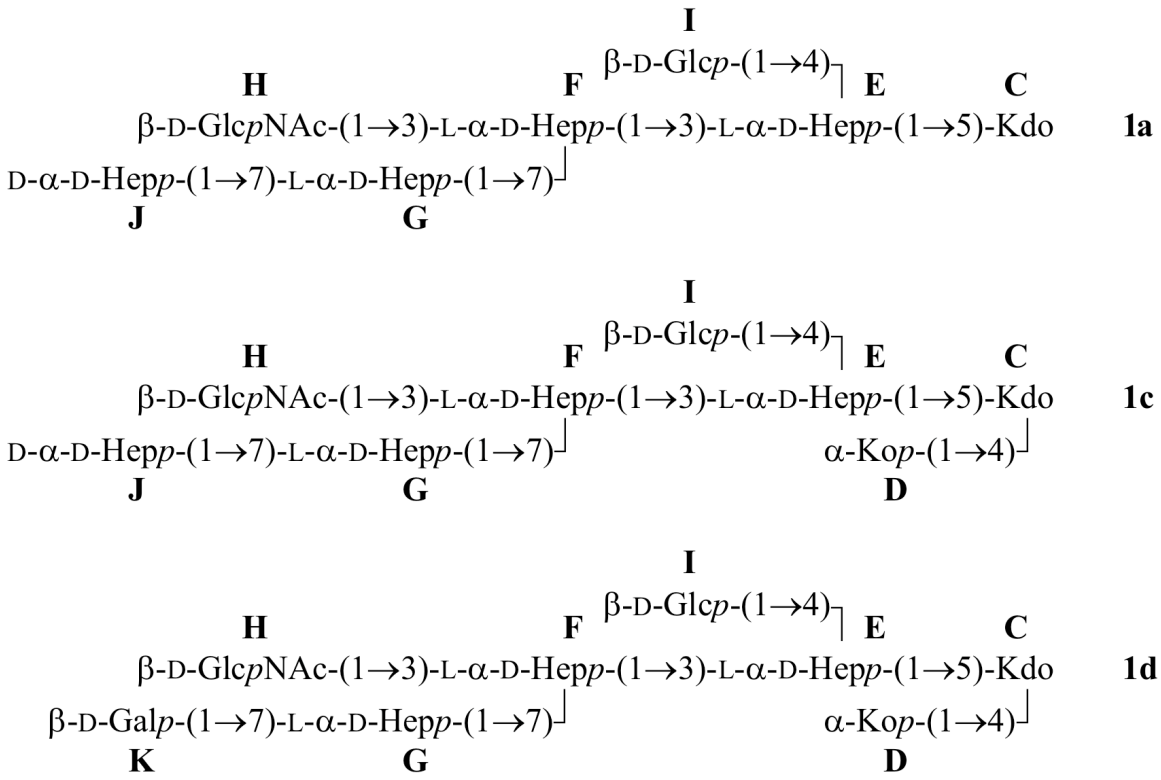

^{1}H NMR spectra of *Yersinia pestis* ssp. *pestis* KM218 core oligosaccharides **1a** (A), borohydride-reduced **1c** (B) and borohydride-reduced **1d** (C). Annotated are anomeric protons in sugar residues denoted by letters as shown above.

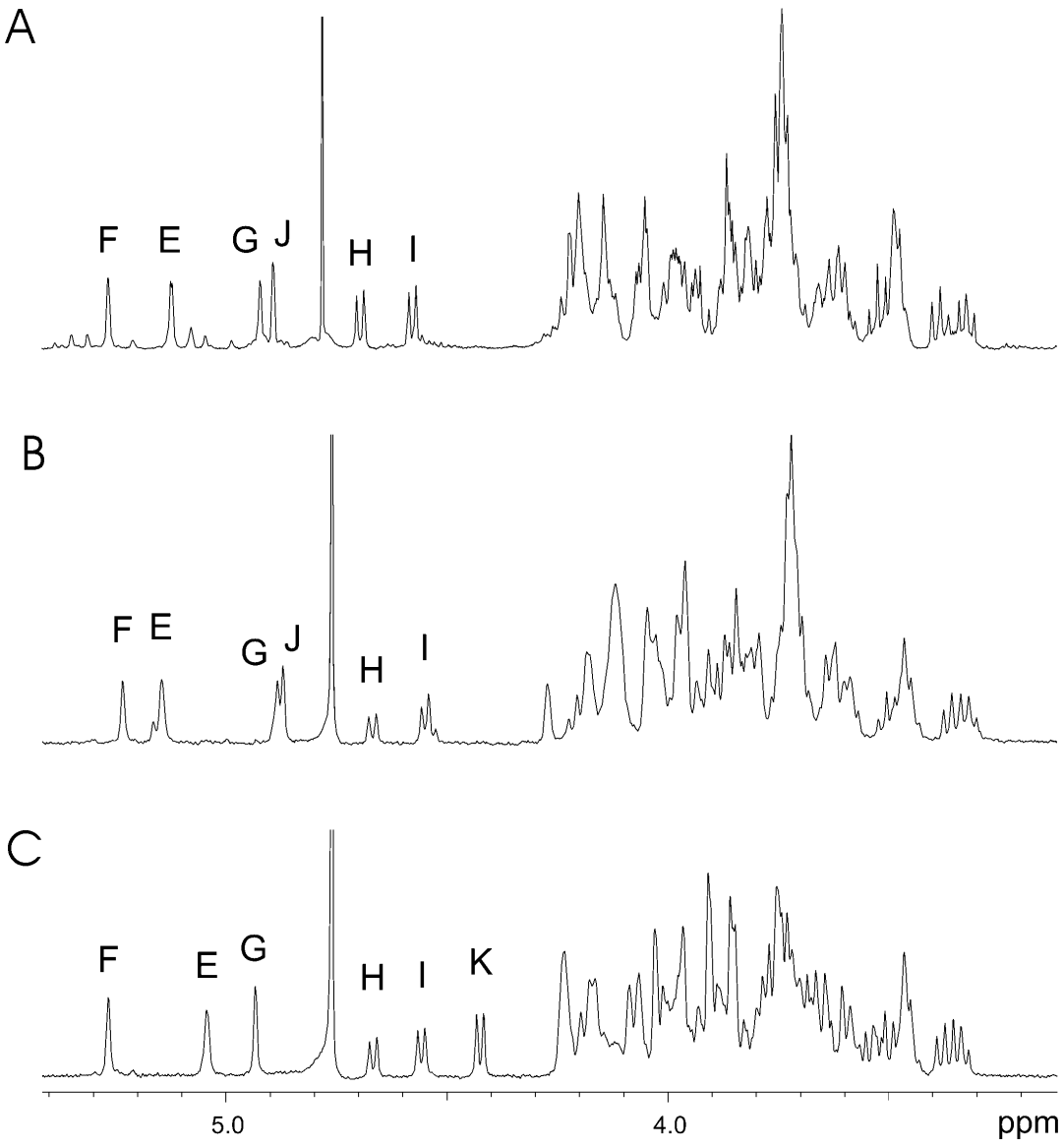

^{1}H and ^{13}C NMR data of *Yersinia pestis* ssp. *pestis* KM218 core oligosaccharides

Sugar residue	Nuc-leus	Chemical shifts (ppm)[a]								
		1	2	3(3a/3b)	4	5	6(6a)	7(7a)(6b)	8(8a)(7b)	8b
Oligosaccharide **1a**										
Kdo **C**	^{1}H		1.88	2.21	4.14	4.16	3.87	3.73	3.60	3.88
	^{13}C			34.6	66.6	75.0	72.1	69.9	64.2	
LD-Hep **E**	^{1}H	5.13	4.06	4.21	4.25	4.22	4.14	3.74	3.74	
	^{13}C	101.3	71.0	76.1	74.4	72.0	69.2	63.8		
LD-Hep **F**	^{1}H	5.27	4.21	4.07	3.94	3.66	4.16	3.66	3.79	
	^{13}C	102.2	68.0	78.6	65.4	73.2	69.1	70.7		
LD-Hep **G**	^{1}H	4.93	4.00	3.87	3.87	3.62	4.21	3.72	3.82	
	^{13}C	101.3	70.7	71.3	66.8	72.5	68.0	70.2		
GlcNAc **H**	^{1}H	4.70	3.76	3.62	3.42	3.50	3.77	3.96		2.07
	^{13}C	99.5	56.5	74.5	70.7	76.6	61.5			23.0
_-Glc **I**	^{1}H	4.58	3.33	3.53	3.39	3.48	3.75	4.01		
	^{13}C	103.2	74.3	76.3	70.6	77.3	62.2			
DD-Hep **J**	^{1}H	4.90	3.98	3.83	3.77	3.66	4.06	3.76	3.84	
	^{13}C	101.1	70.6	71.5	68.1	73.1	72.4	62.4		
Borohydride-reduced oligosaccharide **1c**										
Kdo-reduced **C**	^{1}H		4.12	1.91/2.08	4.04	4.27	3.72	3.63	3.64	3.83
	^{13}C		70.6	37.7	76.8	79.2	73.0	72.8	63.6	
Ko **D**	^{1}H			4.05	3.96	4.12	3.87	4.11	3.70	3.91
	^{13}C			73.4	67.0	69.7	72.6	72.2	63.5	
LD-Hep **E**	^{1}H	5.15	4.02	4.12	4.21	3.97	4.14	3.75	3.88	
	^{13}C	101.4	71.1	75.7	74.8	72.9	69.4	64.3		
LD-Hep **F**	^{1}H	5.23	4.18	4.03	3.89	3.64	4.14	3.72	3.72	
	^{13}C	102.0	68.1	78.9	65.7	72.8	69.4	70.6		
LD-Hep **G**	^{1}H	4.88	3.98	3.84	3.84	3.60	4.18	3.70	3.80	
	^{13}C	101.4	70.7	71.4	67.0	72.7	68.2	70.4		

GlcNAc **H**	^{1}H	4.67	3.74	3.59	3.46	3.47	3.74	3.92		
	^{13}C	99.8	56.5	74.5	70.7	76.6	61.5			
_-Glc **I**	^{1}H	4.55	3.32	3.51	3.36	3.46	3.71	3.99		
	^{13}C	103.2	74.4	76.3	70.8	77.2	62.3			
DD-Hep **J**	^{1}H	4.87	3.96	3.80	3.73	3.73	4.03	3.73	3.81	
	^{13}C	101.2	70.7	71.6	68.2	73.9	72.4	62.5		
Borohydride-reduced oligosaccharide **1d**										
Kdo-	^{1}H		3.99	1.98/2.16	4.19	4.24	3.80	3.59	3.63	3.87
reduced **C**	^{13}C		70.2	38.4	77.1	78.1	71.3	72.4	63.9	
Ko **D**	^{1}H			4.03	3.91	4.09	3.77	4.07	3.70	3.94
	^{13}C			73.2	67.0	69.4	73.0	71.2	63.6	
LD-Hep **E**	^{1}H	5.05	4.07	4.24	4.18	4.02	4.12	3.74	3.84	
	^{13}C	102.5	70.9	75.7	75.0	72.7	69.9	64.5		
LD-Hep **F**	^{1}H	5.27	4.17	4.02	3.89	3.66	4.16	3.75	3.78	
	^{13}C	101.6	68.0	78.9	65.7	73.3	69.3	70.9		
LD-Hep **G**	^{1}H	4.94	3.97	3.86	3.86	3.68	4.23	3.87	3.99	
	^{13}C	101.7	70.8	71.4	66.9	72.5	68.2	72.5		
GlcNAc **H**	^{1}H	4.67	3.74	3.59	3.46	3.47	3.74	3.92		
	^{13}C	99.8	56.5	74.5	70.7	76.6	61.5			
_-Glc **I**	^{1}H	4.55	3.32	3.51	3.36	3.46	3.71	3.99		
	^{13}C	103.2	74.4	76.3	70.8	77.2	62.3			
_-Gal **K**	^{1}H	4.43	3.54	3.65	3.91	3.69	3.74	3.78		
	^{13}C	103.9	71.7	73.4	69.4	76.0	61.8			

[a]Chemical shifts for the N-acetyl group are δ_H 2.07 and δ_C 23.0.

Structure and ^{1}H and ^{13}C NMR data (chemical shifts, ppm) of the Ko-containing core oligosaccharide from the lipopolysaccharide of *Yersinia pestis* ssp. *pestis* EV11M cultivated at 37°C (**2b**)

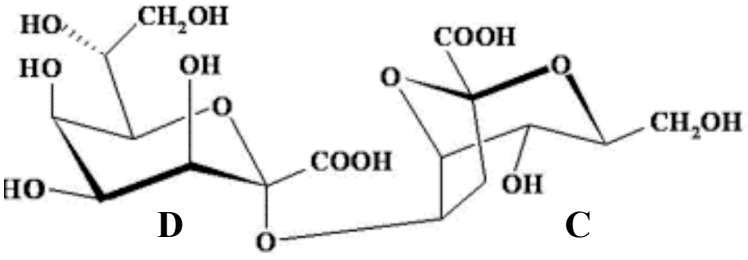

2b

Sugar residue	Nuc-leus	Chemical shifts (ppm)[a]							
		2	3(3a/3b)	4	5	6(6a)	7(7a)(6b)	8(8a)(7b)	8b
2,7-anhydro-Kdo **C**	^{1}H	2.38	2.85	4.66	4.60	3.75	5.54	3.72	3.82
	^{13}C	105.4	44.0	73.3	85.8	63.3	77.3	62.6	
Ko **D**	^{1}H		4.06	4.01	4.16	3.66	4.11	3.80	4.00
	^{13}C	103.4	73.2	67.6	69.8	74.3	71.0	64.9	